CHARACTERISATION AND MECHANICAL PROPERTIES OF NANOCELLULOSE REINFORCED NITRILE BUTADIANE RUBBER GLOVES

Mohamad Nurul Azman Mohammad Taib, Nurhidayatullaili Muhd Julkapli and Wageeh Abdulhadi Yehye

Nanotechnology & Catalysis Research Centre (NANOCAT), Institute of Postgraduate Studies (IPS), University of Malaya, 50603 Kuala Lumpur MALAYSIA

ABSTRACT

Nanocrystalline cellulose (NCC) has been prepared by acid hydrolysis under different concentration of hydrochloride acid (HCl) to verify its crystalline and particle size. The NCC with particle size and diameter less than 150nm ranged was produced with an HCl concentration of 1M, 2M, 3M, 4M and 5M. Furthermore, the infra-red results demonstrated significant changes for region 1059cm^{-1} and bellow 900cm^{-1} , indicated the cleavage of glycosidic linkages of glucose units. The crytallinity index decreased to 59.14% with increased on concentration of HCl up to 5M. Therefore, NCC produced with 1M of HCl demonstrated the highest of thermal stability as reflected in its crystalline index. The addition of NCCs with different pros into Nitrile butadiene rubber (NBR) glove composites demonstrated a substantial increase of mechanical properties in terms of tensile strength, modulus and elongation at break until 5phr but no substantial improvement in tear strength.

BACKGROUND

Cellulose is one of natural carbohydrate that derive from polysachharides that can be found abundantly in nature. Cellulose can be reduced into nano size and is refers as a nano cellulose or nano crystalline cellulose. Nanocystalline cellulose (NCC) is recently has gain attention from researchers and scientists due to some advantages such as with promising mechanical tensile strength (0.3-22GPa), high elastic modulus capacity (58-180 GPa), low density, biodegradability and non-toxicity material. The final properties of NCC are strongly depending on its surface areas, particle size, molecular weight and degree of crystallinity [1-4]. Acid hydrolysis is one of the important routes for mass production of NCC by reduction on the cellulose crystallinity. By using hydrochloric acid (HCl) as a medium for acid hydrolysis in NCC production recorded on a significant increment on the less active surface with less particle size as compared to other types of acid catalysts such as sulfuric acid, bromide acid and phosphoric acid [5-7]. For example, there are some studies on the hydrolysis process of different cellulose sources, that are made from cotton fibers and kenaf by hydrolysed using sulfuric and hydrochloric acid, respectively [8-10]. Synthesis of NCC with HCl as a catalyst, releasing of the hydronium (H+) ion for hydrolytic cleavage of glycosidic bonds in

cellulose molecular chains within amorphous regions brought to the partitioning of the cellulose structures into NCC. By evaluating the parameters of acid hydrolysis process such as concentration of H+ ions, temperature and time would consequently produce NCC with different crystalline, particle size, surface functionalization and geometry. Controlled acid hydrolysis from the cellulose sources disrupts the fibers, breaking the glycosidic chains and breaking up into their constituent rod-like shape or platelet-like figure and form elementary crystalline structure of the NCC.

To date various rubbers have been used to produce rubber gloves such as from natural rubber and synthetic rubber like Nitrile butadiene rubber (NBR) [11]. However this materials alone have some drawbacks such as cannot provide a high enough mechanical properties since the easily to be tearing and lack of tensile strength also not robust to be used. By reinforced with other materials such as carbon blacks, silica, clay, rice bran carbon, nano-Fe_3O_4, zinc dimethacrylate this could provide enhancement in performance such as increase in tear strength, tensile strength, hardness and degradability [12-16]. Although some properties may exhibit a high performance or improvement, there are some limitation of these materials when being used such as lack of environmentally friendly, the decline of modulus of elongation and tensile strength after addition of nano-Fe_3O_4 caused by a large area of phase interface existing between nano-Fe_3O_4 particles [16]. Nanocystalline cellulose (NCC) is a one promising reinforcement agent due to its biologically origin, also have a low density and non-toxicity properties. It is demonstrated that, the final properties of NCC are strongly depending on its surface areas, particle size, molecular weight and degree of crystallinity [1-3]. In the present study, we produced NCCs via acid hydrolysis of cotton linter using hydrochloric acid and then applied the resulting NCCs to reinforce in NBR matrix for preparation of nanocomposite NBR glove with improvement in mechanical execution. This work focused on geometrical, morphology and active surface properties as easily as the purity of NCCs produced with different concentration of HCl. The synthesized NCCs have been characterized in terms of its surface functionality, particle size and crystallinity index. The optimal condition size of NCC in this study was 5M and has been picked out to use as a reinforce filler in Nitrile butadiene rubber to produce rubber composite gloves. This study is required to provide sufficient knowledge about producing NCC with a different concentration of HCl acid to properties of NCC in terms of alterations in chemical characteristics, thermal, size, configuration properties and effects of NCC reinforcement on mechanical properties of NBR glove composites produce.

2.0 MATERIALS AND METHODOLOGY

Commercial available cotton linter Microcrystalline cellulose (MCC) with a diameter of size 20 ųm, HCl 37 wt. %, NBR latex and chemicals was purchased from Friendemann Schmidt and local providers.

2.1 Synthesis and Preparation of NCC

MCC (5g) was manually mixed at different concentration of HCl acid (1M, 2M, 3M, 4M and 5M). The mix was then hydrolyzed at 100°C for 60min, with continuous stirring (500 rpm) in a conical flask. After completed the mixture was quenched in ice tube to check the reaction. The reaction mixture then was rinsed with distilled water and centrifuged for 30 minutes at 3000 RPM, using repeated centrifugation. The supernatant was transferred from the sediment and replaced by new distilled water and centrifuged again for five times. The product then was dialysis using a dialysis tube by using distilled water until the pH of water was constant at pH 7. The resulting suspension was then freeze dried and stacked away at room temperature before further processing and compounding in matrix.

2.2 Preparation of NBR/NCC Glove Composites

For NBR/NCC glove composites, the NCCs (5M HCl) was chosen as a reinforce filler in composites. A desired content of dried NCCs was mixed with NBR latex and stirred vigorously at room temperature for 30minutes. And so, the compounding of NBR/NCC with other ingredients was carried away in a beaker with a stirrer. The glove of NBR/NCC composites was prepared using a dipping tank method. The former used was produced from ceramic. The NBR/NCC glove composites was cured by oven at 125°C for 20 minutes. By modifying the contents of NCCs over the range of 0phr, 1phr, 2phr, 3phr, 4phr and 5phr, a series of NBR composites with thickness around 8mm were prepared and coded as NBR control, NBR/NCC 1phr, NBR/NCC 2phr, NBR/NCC 3phr, NBR/NCC 4phr, and NBR/NCC 5phr respectively.

2.3 Characterization

2.3.1 Fourier Transform Infra Red (FTIR) Spectra analysis

FTIR spectra were recorded on a Thermo Nicolet FTIR spectrometer (Nicolet 6700, USA) in the range of 400-4000cm^{-1} with a spectral resolution of 4cm^{-1} and 32scans for each sample were recorded. Each sample was palletized with KBr powder.

2.3.2. X-Ray Diffraction (XRD) Analysis

X-ray diffractometer (XRD) data were collected using X-ray diffractometer equipped with Cu Kα radiation (λ=0.1541nm) at the operating voltage and current of 45kV and 100 MA, respectively. Diffractograms were collected in a 2θ range of 5~40 at a rate of 1°/min with a resolving power of 0.05°.

The crystallinity index was forecast as follows in Eq. (2):

$$\mathrm{CrI} = \frac{I_{002} - I_{am}}{I_{002}} X\ 100 \qquad (2)$$

Where I_{002} is the overall intensity of the peak at 2θ about 22° and I_{am} is intensity of baseline at 2θ about 18°.

2.3.3 Transmission Electron Microscopy (TEM) Analysis

Drops of 0.001% of NCC suspensions were deposited on glow-discharged carbon-coated TEM grids. The specimen were then negatively stained with 2% uranyl acetate, prior to complete drying and observed using a Philips CM200 electron microscope operating at 200kV. Images were recorded on Kodak SO163 films.

2.3.4 Mechanical Tests

The tensile test was carried out by using Universal Testing Machine. The samples were cut in dog bone shape. All experiments were held out at room temperature with a crosshead speed of 500mm/min according to ASTM D412. Tear test was taken according to ASTM D624.

3.0 RESULTS AND DISCUSSION

3.3 Fourier Transform Infra-Red (FTIR) Analysis

Fig. 3 (a) shows the FTIR for NCC synthesized under different concentration of acid catalyst. The strong, broad band was observed for 3500cm^{-1} region due to O-H bonds stretching vibration. This band consists of intra and inter-hydrogen bonds between the NCCs. O-H bonds broadband was largely increased for NCC samples synthesized with 1M to 5M HCl. The high density of hydroxyl groups could be corresponding to this peak due to more active surface on NCCs. This means more capable active surface to establishing hydrogen bonding with water/moisture molecules, thus indicating the existence of hydroxyl groups or highly hydrogen bonded network. The C-H is stretching, vibration intensity 2900 cm^{-1} was prominent with increase the acid concentration (1M to 5M) due to the presence of $–CH_2$ moieties in the NCC samples. 1644cm^{-1} (Fig. 3 (b)) band that associated with O-H bending of absorbed water from moisture more intense with increased the molar concentration of acid used from 1M to 5M and was stronger for NCCs compared to control MCC because due to larger surface area of NCCs compared with MCC. Althought the NCC samples were subjected to proper dring using freeze drying method, the elimination of water was difficult due to water to NCCs interaction. The presence of 1433cm-^{1} due to CH_2 bending motion in cellulose, the presence of this peak also was suggested due to active side of intermolecular hydrogen attraction of C6 group. The band at 1372 for MCC shifted to 1370cm^{-1} after hydrolysis with acid due to C-H bending or assymetric C-H deformation, the band at 1332 cm^{-1} for MCC shifted to 1329 cm^{-1} (1M), 1328 cm^{-1} (2M), 1328 cm^{-1} (3M), 1327 cm^{-1} (4M) and 1327 cm^{-1} (5M) due to CH_2 wagging, 1164 cm^{-1} due to C-O anti symmetric stretching, 1115cm^{-1} shifted to lower band at 1113 cm^{-1} after hydrolysis was due to C-O and C-C stretching. The sharp peak observed at 1058 cm^{-1} (MCC) to 1059cm^{-1} (after hydrolysis with 5M HCl) due to C-O-C pyranose ring stretching vibration. Increase on this band would associate with increment of cellulose content. The band at 897 cm^{-1} associate with β-glycosidic linkages consist of C_1-H and O-H bending of typical cellulose structure.

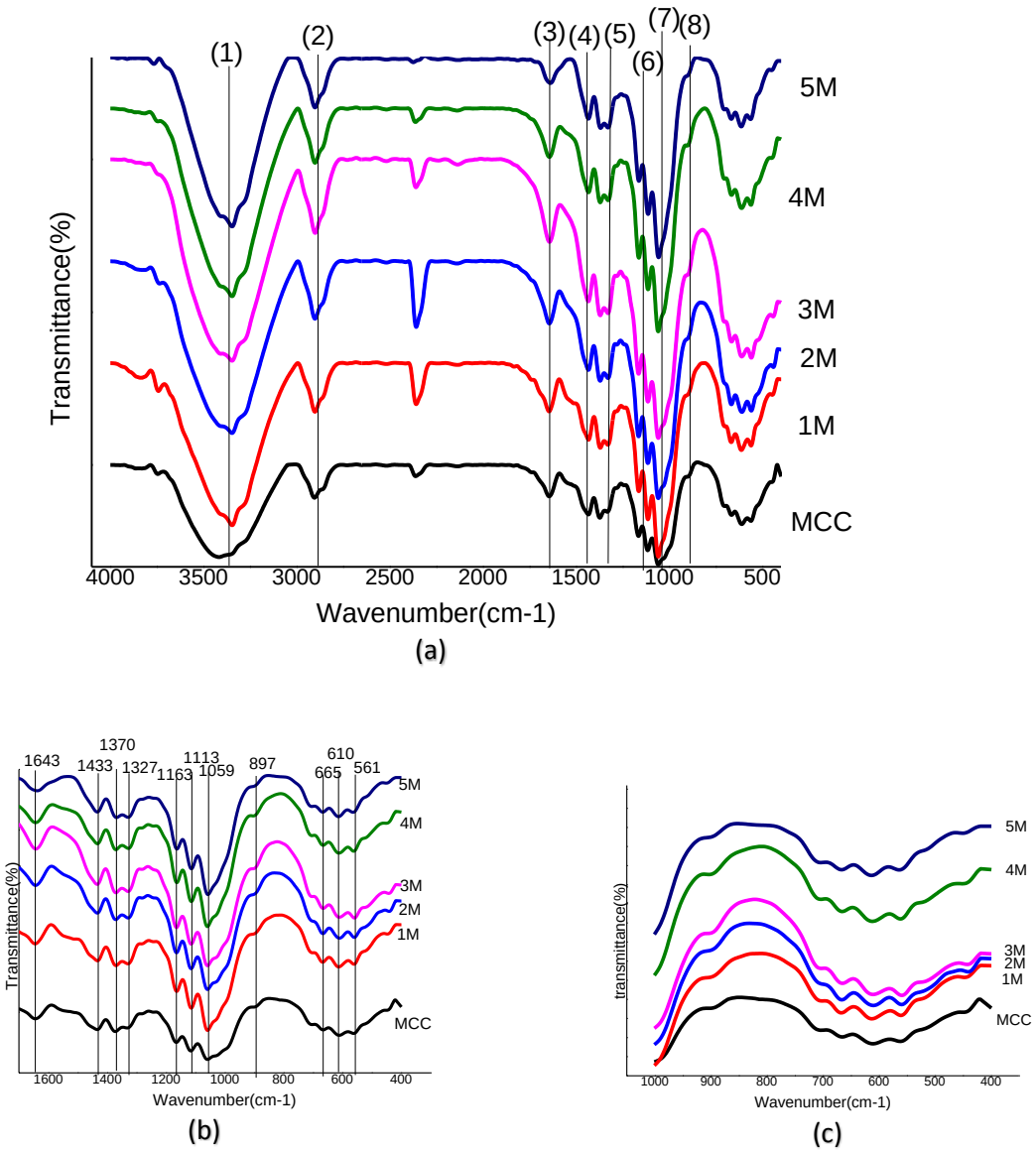

Fig. 3. FTIR for MCC and NCCs (a) 4000-400cm^{-1} ;(b) 1700-400cm^{-1}; (c) 900-400cm^{-1}

In general, the hydrolysis of NCC does not directly separate crystallites that are laterally bound by secondary interaction. However, a hydrolysis carried out by harsher condition shortens the crystallites, thus facilitating the separation. 1058cm^{-1} -1059cm^{-1} was assigned to ether groups and also β-glycosidic linkages. This band more prominent with increased of molar concentration that indicated the formation of ether groups and cleavages in sugar units. 894cm^{-1} was assigned to glycosidic linkage between glucose units. This small band cannot be observed directly with the acid concentration changes. However, as concerned to region bellow 900cm^{-1} (Fig. 3 (c)), it was clearly changed with the concentration of acid used increased from 1M to 5M. This band also became more narrowed with increased the molar

concentrations that were due to reduction in breakdown of the glycosidic linkage to glucose units. In Table 1 shows the assignments of the FTIR bands.

Table 1
Infrared spectra with assignments of different bands

No	Band position cm-1	Band assignments
1	3416-3346	O-H stretching, vibration (hydrogen bonded)
2	2901-2904	C-H stretching vibration
3	1642-1644	Adsorbed water or moisture
4	1370	C-H bending or assymetric C-H deformation
5	1327-1332	C-H deformation and C-OH deformation
6	1164	C-O-C asymmetric valence vibration
7	1058-1059	C-O ether vibrations, methoxyl and β-O-4
8	897	C-H out of plane in position ring stretching in cellulose due to β-linkage

3.4 X-Ray Diffraction (XRD) Analysis

The main peaks of all samples appeared at 14.7, 16.6, 22.8 and 34.1^{o} (Fig.4), attributed to the diffraction planes of (101), $(10\bar{1})$, (200) and (400), respectively [17]. This pattern is similar to native cellulose or cellulose I. Cellulose I is most abundant form found in nature [18]. Cellulose I content of two distinct crystalline forms that are cellulose Iα (triclinic) and cellulose Iβ (monoclinic). The amount of these both cellulose I are dependent on the source of cellulose and usually cellulose Iβ is dominant in plant. peaks at (101) and $(10\bar{1})$ would more pronounced when the crystalline content is high. This suggested that the acid hydrolysis using HCl had a limited effect on the polymorphism of cellulose I for the NCC sample produced. Further understand of crystal structure, the samples crystallinity were calculated by using Eq. (1) and presented in Table 2. It was shown that the acid hydrolysis process by using high concentration would decrease the crystallinity of the NCC produced. High concentration of acid used would result in a faster hydrolysis of NCC by harsher treatment. A hydrolysis process was carried out by harsher condition shortens the polymeric chains of NCC and promotes more crystallite structures. Thus some degradation of crystalline part occurred during the hydrolysis condition The NCC crystallinity produce was decreased as the concentration H+ ions increased during the hydrolysis process. The

reduction on the diffraction intensities of the amorphous region around 18° attributed to the less ordered region of NCC polymeric chains. The water holding capacity of NCC was related to its crystallinity as the amount of freezing bound water decreases with increasing degree of crystallinity within the NCC molecules [19, 20]. Moreover, the X-ray diffraction patterns reflected decrease in the crystalline domains in the NCC as a function of acid hydrolysis (Fig. 4). This was evidenced by the significant decreased intensity of diffraction peak at 22.8^{o}.

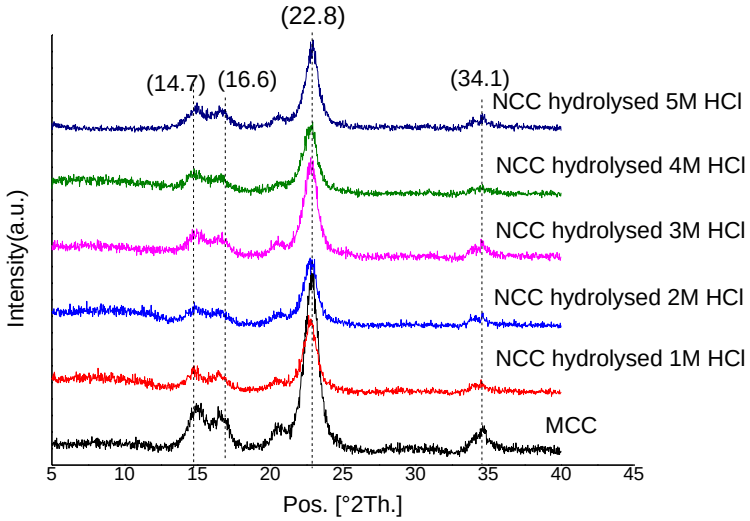

Fig. 4. XRD of MCC and NCCs (1M to 5M)

Table 2
X-ray Diffractogram Crystallinity Index for different types of NCC

Type of sample	Crystallinity index
MCC	76.10
NCC hydrolysed with 1 M HCl	72.51
NCC hydrolysed with 2 M HCl	69.19
NCC hydrolysed with 3 M HCl	63.44
NCC hydrolysed with 4 M HCl	59.28
NCC hydrolysed with 5 M HCl	59.14

3.5 Transmission Electron Microscopy (TEM) Analysis

Transmission electron micrographs of the MCC and NCCs are shown in Fig. 5a to 5e, respectively. MCC morphology in Fig. 5a shows that the large dimension with some color contour from dark to white. The dark part indicated the thicker size compared to the white part. This was due to agglomeration between the MCC. Meanwhile, Fig. 5c shows most probably the needle-like and narrow-like shapes and indicated that treatment with 2M of HCl would hydrolyze more about MCC into NCC with different variety of size and shapes. Treatment with 3M of HCl start to turn and change the shape of NCCs produced from the platelet-like shapes to smaller particulate size with no significant variation. The differentials of shapes were observed as 5M, 4M, 3M, 2M and 1M acid catalysts were used and compared. The NCCs after hydrolyzed by acid were found to form aggregated due to hydrogen bond interactions via the surface hydroxyl groups. The platelet-like particles of the NCC were more observed especially at higher concentration of acid (Fig. 5d, Fig. 5e and Fig. 5f). The effect of interfacial interaction and bond ability between NCC through hydrogen bonding could be amplified by the larger specific surface area of the NCC. The specific surface area would be increased with increasing aspect ratio or decreasing diameter of NCC. The NCC which have larger surface to volume ratio could provide more contact surface with polymer matrix for improving surface reactivity which enabling to more effectively impede the polymer chains mobility [21]. By increasing interfacial interaction the better molecular level distribution and the improved properties of composite by using rather low filler content could be expected. However, the high surface area of these nano sized cellulose might draw the surrounding nano sized cellulose together to be agglomerate driven by their high hydrophilic nature when dried [22]. When aggregation occured it was difficult to be re-dispersed, thus the NCC is not suitable for reinforcement purpose without any modification treatment or functionalization.

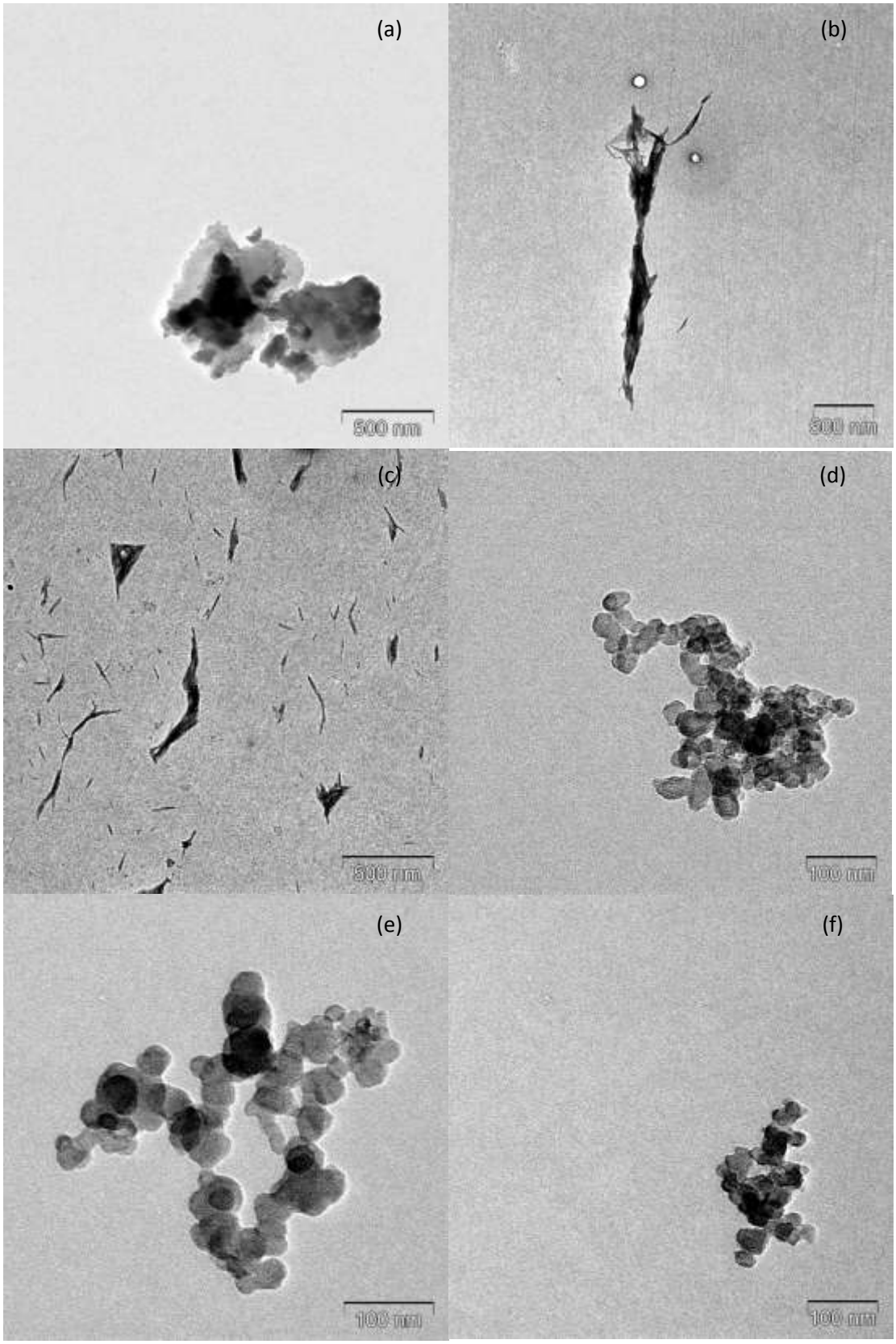

Fig. 5. TEM images of **(a)** MCC (500nm), **(b)** 1M(200nm), **(c)** 2M(200nm), **(d)** 3M(100nm),**(e)** 4M(100nm), **(f)** 5M(100nm)

3.7 Mechanical Properties

The mechanical performance of NCC/NBR is demonstrated in Table 4. For tensile strength result shows some improvement with NCCs addition in NBR composites from 1phr to 5phr, the slight decrease of 2phr when compared with control was caused by the incompatibility or agglomerated of NCC in NBR matrix, but this decrease was not significantly when compared to each other. The tensile strength for 4phr and 5 there were higher when compared to NBR control sample. Even though mean of 5 there was the highest, there was no substantial difference between mean of 5 phr with 4 per result, this suggested that 4phr was the optimal condition for addition NCC in NBR matrix. Different studies by [11] on foamed nitrile rubber reinforced with cellulose nanocrystals suggested that the 15phr with value of 6.54Mpa is optimum to be filled in nitrile foam rubber due to foamed rubber has many voids, it's suggested that the smaller the foam size, the better mechanical properties of foamed rubbers. The low loading NCC filler in matrix can improve the mechanical properties as suggested by [11, 23].

Table 4
Mechanical properties of NCC reinforced NBR composites

NCCs content (phr)	Tensile strength (MPa)	Modulus at 100% strain (MPa)	Modulus at 300% strain (MPa)	Modulus at 500% strain (MPa)	Elongation at break (%)	Tear Strength (kN/m)
0	8.264(1.07)	1.057 (0.18)	1.346(0.28)	1.680(0.48)	3.457(0.65)	15.008 (1.85)
1	8.780(0.78)	0.871 (0.08)	1.213(0.09)	1.646(0.12)	2.937(0.32)	14.714 (1.23)
2	7.259(1.46)	0.840 (0.03)	1.106(0.04)	1.402(0.06)	2.807(0.14)	14.808 (1.61)
3	9.105(2.15)	0.983 (0.06)	1.272(0.09)	1.674(0.11)	3.315(0.23)	14.020 (0.78)
4	13.608(1.65)	1.173 (0.04)	1.909(0.07)	3.392(0.14)	3.504(0.13)	13.106 (0.74)
5	16.588(3.06)	1.597 (0.11)	2.753(0.22)	5.408(0.42)	4.539(0.34)	15.458 (1.21)

*** Standard deviations are shown in brackets**

The effects of NBR composites on tensile modulus stress at 100% of elongation (M100) was shown in Table 4. Results indicated that the M100 increased with the increasing of NCCs content from 1 phr to 5 phr, there was significant different between the groups but this significant value only at 5phr as compared to others. No significant increment when compared from NBR (control) and 1phr to 4phr. The increment of Modulus at 100% (M100) for 1phr to 5 there was due to improvement of cross-linking in NBR matrix with NCC. The incorporation of NCCs into the NBR matrix increased the stiffness because the tensile modulus represents the material stiffness. Better dispersion could enhance the interfacial adhesion between NCCs and NBR matrix, interfacial adhesion between NCCs and NBR occurred as shown in a morphological study could suggest that the NCC create hydrogen bonding between each other that affected on the interfacial bond between NCC and NBR matrix. No significant increment of Modulus at 300% and 500% at 1phr to 3phr when compared with NBR (control). The addition between 1phr to 3phr didn't have any effects on cross linking between NBR networks thus not promote any improvement. The increment stated to significantly improve at 4 phr and 5phr of NCC addition. This was due to strong network interactions between rubber and filler has been formed. In Table 4 also shows the elongation at break for NBR and NBR composites at difference phrs. From the results in Table 4 showed that the 5 phr NCCs loading had the highest elongation at break and 2 phr has the lowest elongation at break. Addition of 5phr could improve the elongation at break for NBR. This could be caused by the better cross linking between NBR and NCCs. The result indicated that from 1phr to 4phr, no significant results were obtained when compared with NBR (control). This was due to the fact that the addition of NCC at 1phr to 4phr created the agglomeration between NCCs in matrix due to strong hydrogen bonds interaction between NCCs, thus create a brittle form on NBR thus lowering the elongation at break and no improvement could obtain. An interactions were formed between rubber chains and NCCs would decrease the ability to resist deformation on rubber chains itself. A flexibility and elasticity of the rubber chain were less and restricted when NCCs were incorporated into NBR matrix, which resulted in a more rigid rubber matrix and reduce the elongation at break. The tear strength result in Table 4 was not significantly different with increment of different levels of phr between each other. Even though the mean results showed some improvement with increment up to 5 phr but the standard deviation was not significantly different between other samples. The addition of cellulose in nano size cannot stop the propagation of a crack that initiated by the tearing force. This could be due by lack of interaction between NBR and NCCs that can stop the intial propagation of crack in matrix when forces was applied.

4.0 CONCLUSION

NCC was successfully extracted by hydrolysis of commercial microcrystalline cellulose cotton linter. The effect of HCl concentration had been studied and obtained NCC materials were compared with particle size, functional groups and crystalline phase. It found the size was reduced with increasing the concentration of acid, contributed by more hydrolysed on cellulose polymer chains. Particle size of NCC reduced till 10 to 15 % as the concentration of HCl used for hydrolysis process was increased from 1 M to 5 M. The crystallinity of NCC demonstrated some degree of reduction due to the more predominant of glycosidic linkage break down. Furthermore, higher concentration of HCl used tends to obtained NCC with more particulate nuances rather than colloidal suspension. The effects of NCC addition to different loading of them were investigated and the results can be concluded that the maximum strength could be obtained is 4phr and no significant improvement in tensile strength up to 5phr. The NBR composites produced with reinforcement of NCC can be used to improve the performance of some mechanical properties.

5.0 Acknowledgement

The authors would like to thank to Ministry of Science and Technology (MOSTI) Malaysia for financial support of this project. This project was financially supported by Science Fund (***SF013-2013: Modification of NCC for production of NCC polymer and rubber composite***).

References

[1] S. Elazzouzi-Hafraoui, Y. Nishiyama, J.-L. Putaux, L. Heux, F. Dubreuil, C. Rochas, Biomacromolecules. 9 (2007) 57-65.
[2] B. Peng, N. Dhar, H. Liu, K. Tam, Can. J. Chem. Eng. 89 (2011) 1191-1206.
[3] S. Rebouillat, F. Pla, J Biomater Nanobiotechnol. 4 (2013) 2.
[4] K.-Y. Lee, Y. Aitomäki, L. A. Berglund, K. Oksman, A. Bismarck, Compos. Sci. Technol. 105 (2014) 15-27.
[5] M. L. Yan, S. J. Li, M. X. Zhang, C. J. Li, F. Dong, W. Li, BIORESOURCES. 8 (2013) 6330-6341.
[6] Y. J. Tang, S. J. Yang, N. Zhang, J. H. Zhang, *Cellulose.* 21 (2014) 335-346.
[7] H. Sadeghifar, I. Filpponen, S. P. Clarke, D. F. Brougham, D. S. Argyropoulos, J. Mater. Sci. 46 (2011) 7344-7355.
[8] H. Kargarzadeh, I. Ahmad, I. Abdullah, A. Dufresne, S. Zainudin, R. Sheltami, *Cellulose.* 19 (2012) 855-866.
[9] L. H. Zaini, M. Jonoobi, P. M. Tahir, S. Karimi. J Biomater Nanobiotechnol. 4 (2013) 1.
[10] T. F. Meyabadi, F. Dadashian, G. M. M. Sadeghi, H. E. Z. Asl, Powder Technol. 261 (2014) 232-240.
[11] Y. Chen, Y. Zhang, C. Xu, X. Cao. Carbohydr. Polym. 130 (2015) 149-154.
[12] C. H. Xu, Y. K. Chen, Y. P. Wang, X. R. Zeng, Polym. Compos. 32 (2011) 2084-2092.
[13] A. Mostafa, A. Abouel-Kasem, M. R. Bayoumi, M. G. El-Sebaie. Mater. Des. 30 (2009) 2721-2725..
[14] S. I. Volfson, N. A. Okhotina, A. I. Nigmatullina, O. A. Panfilova. *AIP Conference Proceedings.* 1599 (2014) 418-421.
[15] S. H. Xu, J. Gu, Y. F. Luo, D. M. Jia, L. Yan, Polym. Compos. 36 (2015) 861-868..
[16] Q. L. Wang, F. Y. Yang, Q. Yang, J. H. Chen, H. Y. Guan, Mater. Des. 31 (2010) 1023-1028.
[17] P. Mansikkamäki, M. Lahtinen, K. Rissanen. Carbohydr. Polym. 68 (2007) 35-43.
[18] S. Park, J. O. Baker, M. E. Himmel, P. A. Parilla, D. K. Johnson, Biotechnol. Biofuels. 3 (2010) 10.
[19] K. Nakamura, T. Hatakeyama, H. Hatakeyama. Text. Res. J. 51 (1981) 607-613.
[20] A. Espert, F. Vilaplana, S. Karlsson, Compos. Pt. A-Appl. Sci. Manuf. 35 (2004) 1267-1276.

[21] M. Minelli, M. G. Baschetti, F. Doghieri, M. Ankerfors, T. Lindström, I. Siró, D. Plackett. J. Membr. Sci.358 (2010) 67-75
[22] P. Lu, Y.-L. Hsieh, Carbohydr. Polym. 82 (2010) 329-336.
[23] X. Cao, C. Xu, Y. Wang, Y. Liu, Y. Liu, Y. Chen, Polym. Compos. 32 (2013) 819-826.